Negative Interest Rate Policy and Yield Curve*

Jing Cynthia Wu
Chicago Booth and NBER

Fan Dora Xia
Bank for International Settlements

First draft: January 17, 2017
This draft: December 20, 2017

Abstract

We extract the market's expectations about the ECB's negative interest rate policy from the yield curve and study its impact on the yield curve. To capture the rich dynamics of the short end of the yield curve, we introduce two policy indicators, which summarize the immediate and longer-horizon future monetary policy stances. The ECB has cut interest rates four times under zero. We find the June 2014 and December 2015 cuts were expected the month before, and the September 2014 cut was unanticipated. Most interestingly, the March 2016 cut was expected 4 months before the actual cut.

Keywords: negative interest rate policy, effective lower bound, term structure of interest rates, shadow rate term structure model, regime-switching model

*This article was formerly titled "Time-Varying Lower Bound of Interest Rates in Europe." We thank Drew Creal, Felix Geiger, Jim Hamilton, Wolfgang Lemke, Eric Swanson, and seminar and conference participants at UCSD Rady School of Management, University of Oxford, 10th Annual Conference of the Society for Financial Econometrics, the Federal Reserve Board's conference on "Developments in Empirical Monetary Economics," the 7^{th} Term Structure Workshop at Bundesbank Bank, "European Central Bank, University of Illinois Urbana-Champaign, Texas A&M University, Tilburg University, Banque de France, Tinbergen Institute, University of Copenhagen, Universite Catholique de Louvain , and BIS Asian office for helpful suggestions. Cynthia Wu gratefully acknowledges financial support from the James S. Kemper Foundation Faculty Scholar at the University of Chicago Booth School of Business. The views expressed herein are those of the authors and not necessarily the views of the BIS. Correspondence: cynthia.wu@chicagobooth.edu, dora.xia@bis.org.

1 Introduction

The effective lower bound (ELB) of nominal interest rates is one of the most discussed economic issues of the past decade. The negative interest rate policy (NIRP) is among the latest additions to unconventional monetary policy toolkits, in the hopes of providing further stimulus to the economies that face the ELB. For example, in June 2017, the deposit rate of the Swiss National Bank was at a record low of -0.75%, while the European Central Bank's (ECB) deposit facility rate was -0.4%.

As an emerging policy tool, it is important for policy makers and economists to understand its implications. First, the total value of outstanding government bonds with negative interest rates had reached 10 trillion dollars by the end of 2016 and is still growing due to the NIRP. The question is, what is the NIRP's impact on the yield curve? Second, what are economic agents' perceptions of this policy and how do they form expectations? Third, because the zero lower bound (ZLB) is no longer binding, the NIRP creates richer shapes for the short end of the yield curve. How do we accommodate them when we model the term structure of interest rates? Understanding these questions is important to European countries and Japan, which are currently implementing the NIRP. Such an understanding is also potentially important for the US economy, for which the NIRP remains a future option if large negative shocks hit the economy.

We propose a new shadow rate term structure model (SRTSM) to address these questions, and we focus on the Euro area. At the ELB, the short end of the yield curve displays three different shapes. The first case is flat as we see in the US data when the ZLB prevails but not the NIRP. Second, the yield curve could be downward sloping when agents expect future cuts of the policy rate due to the NIRP. Third, in some days, it is initially flat in the very short end and then downward sloping, implying market participants expect no immediate action from the central bank, but they think the overall future monetary policy is expansionary. To capture these shapes, we introduce two policy indicators: one for the immediate monetary policy stance, and the other for the future monetary policy stance in longer horizons. We

model the discrete movement of the relevant policy rate, the ECB's deposit facility rate, at the ELB with a simple and intuitive regime-switching model conditioning on the two policy indicators. Our model is able to capture the three different shapes of the yield curve we see in the data. We then build the dynamics of the deposit rate into an SRTSM using the Black (1995) framework, where the short term interest rate is the maximum of the non-positive deposit rate and a shadow interest rate.

We use our model to extract the market's expectations on the NIRP. Overall, expectations of financial market participants from our model agree with economists' expectations from the Bloomberg survey. Importantly, our model has the advantage over the Bloomberg survey because we can extract the market's expectations further into the future, whereas the Bloomberg surveys are collected only one week before monetary policy meetings. We find the June 2014 cut and December 2015 cut were expected the month before, and the September 2014 cut was entirely unanticipated. Most interestingly, the March 2016 cut was expected 4 months before the actual cut.

We then evaluate the NIRP's impact on the yield curve by conducting some counterfactual analyses at the end of our sample in June 2017. First, we ask what would happen to the yield curve, if the ECB indicated an easing position in the next meeting, but promised this cut would be the last one in history. In response to such an announcement, the yield curve would shift down by about 0.03% across all maturities. Second, what if the central bank announced it would not make any move in the next meeting, but the overall future environment would be expansionary? The one month rate would not decrease, but yields at other maturities would. The change would grow with the maturity up to two years, and then flatten out afterwards at about 0.1%. Third, suppose the ECB communicated with the public about its expansionary plan across all horizons. This action would amount to the largest changes. The change at the one month horizon would be 0.03%, it would increase when maturity increases, and the largest change would happen at the 2 year horizon, amounting to 0.2%. The size of the change would decrease to about 0.16% in the long run.

The term structure model allows us to decompose long term yields into expectations and term premium. Our model-implied 10-year term premium increased between 2005 and 2008. It has trended down since 2009, and became negative at the ELB, potentially due to QE purchases. The dynamics of the deposit rate contributes positively to the premium, but in a smaller order of magnitude.

We compare our model to several alternatives including several SRTSMs proposed in the literature and the Gaussian affine term structure model (GATSM). We find our new model performs the best in terms of higher likelihood and lower pricing errors. The existing models in the literature, on the other hand, do poorly.

After a brief literature review, the rest of the paper proceeds as follows. Section 2 motivates and models the dynamics of the deposit rate, and Section 3 sets up the new SRTSM. Section 4 discusses data, estimation, and estimates. Section 5 turns to model implications regarding the NIRP, while Section 6 focuses on yield curve implications. Section 7 concludes.

Literature Earlier work has applied the SRTSM mostly to the Japanese and US yield curve. For example, Kim and Singleton (2012) and Ichiue and Ueno (2013) focus on Japan, whereas Krippner (2013), Christensen and Rudebusch (2014), Wu and Xia (2016), and Bauer and Rudebusch (2016) focus on the United States. These papers kept the lower bound at a constant level.

A few studies have worked on the new development in Europe, where the policy lower bound kept moving down to negative numbers after the NIRP. For example, the online implementation of Wu and Xia (2016) for the Euro area, and Lemke and Vladu (2016) and Kortela (2016). However, none of these papers allow agents to be forward-looking in terms of the future movement of the policy rate, which is an important feature of our model. And this feature allows our model to fit the short end of the yield curve much better than the ones in the literature.

Our paper relates to the regime-switching literature, with the seminal paper by Hamilton

(1989). Applications of this class of model in the term structure literature include Ang and Bekaert (2002), Bansal and Zhou (2002), and Dai et al. (2007). These papers allow the parameters of the dynamics to take several different values. More related to our paper, Renne (2012) allows the monetary policy rate to take discrete values and follow a regime-switching process. The difference is we build the regime-switching model for the policy rate only when ELB is binding. Otherwise, the state variables follow a Gaussian vector autoregression (VAR) as in the literature. The advantages of our model are twofold. First, it significantly reduces the state space for the regime-switching process. Second, when the ELB is not binding, our model is essentially the GATSM, which is the preferred model in the literature.

2 NIRP

2.1 Rate cuts and yield curve

Since the deposit rate hit the ELB in July 2012, the ECB has adopted the NIRP and further cut rates four times. To understand whether these cuts were anticipated by the market, Figure 1 plots the yield curves the months before these cuts. June 2014 was a historical moment in which the ECB cut the deposit rate to negative for the first time. The ECB made efforts to communicate with the public prior to the event. By May 2014, the market did expect a rate cut going forward, but it did not fully digest the cut of 0.1% in the next month. Instead, it expected a cut of 0.1% within three months. The second cut was entirely unexpected, and the yield curve was basically flat in August 2014. The December 2015 cut was fully anticipated. Moreover, in November 2015, the market expected further cuts beyond the next meeting, and expected a total of a 0.2% cut in the next year. In February 2016, the market anticipated further cuts, with the total scale over 0.2%.

Figure 1: Yield curves before rate cuts

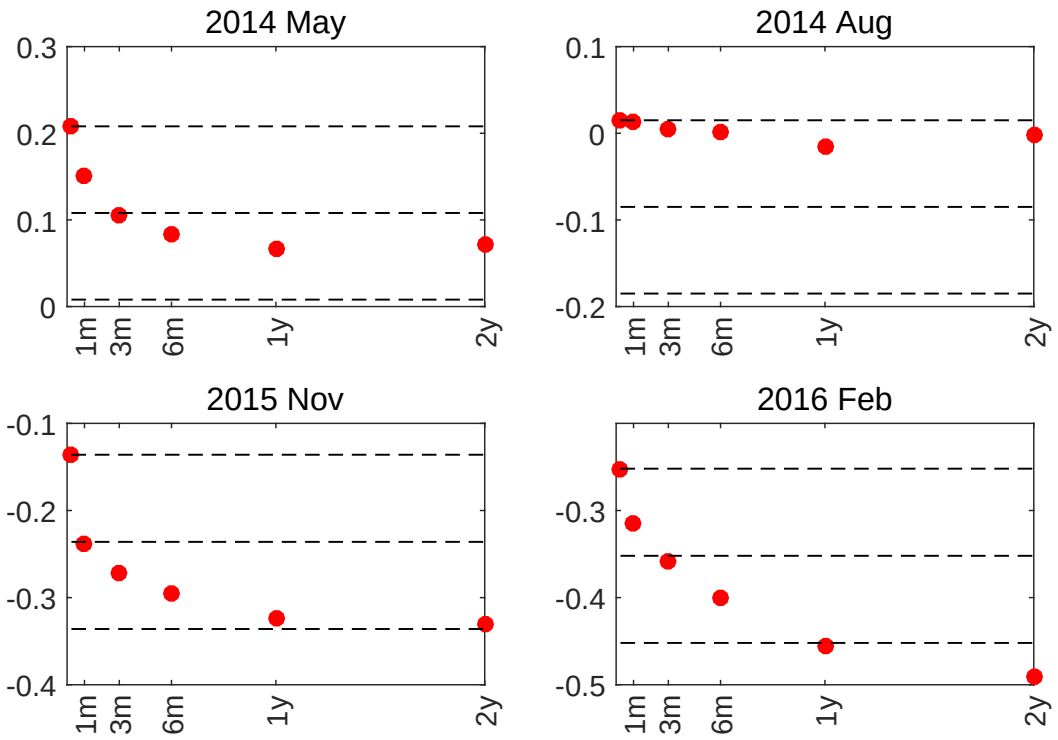

Notes: Yield curves on May 2014, August 2014, November 2015, and February 2016. Red dots: observations. Black dashed lines mark the short rate, short rate - 0.1%, and short rate - 0.2%. X-axis: maturity. Y-axis: interest rates in percentage points.

2.2 Modeling the short end of the yield curve

The NIRP introduces richer dynamics for the short end of the yield curve. See the red solid dots in Figure 2. In July 2013, the front end of the yield curve was flat. This flatness was the basic pattern we see in the data when the US experienced the ZLB. Most efforts in the term structure literature for the ZLB focus on this feature; see, Christensen and Rudebusch (2014), Wu and Xia (2016), and Bauer and Rudebusch (2016). However, the NIRP introduced additional patterns: in both February 2016 and July 2016, the yield curves were downward sloping, implying future decreases in the policy rate. Interestingly, the very short ends for the two months are different: in February 2016, an easing future monetary policy stance was expected throughout all horizons, whereas in July 2016, the very short

Figure 2: Yield Curves

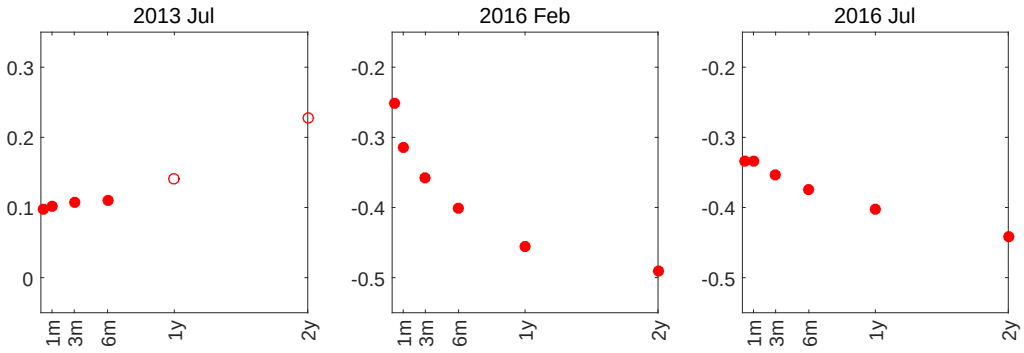

Notes: Yield curves in July 2013, February 2016, and July 2016. X-axis: maturity. Y-axis: yield in percentage points. Red solid dots correspond to ELB.

ends of the curve was flat, suggesting the cut would not happen in the next month.

We build a simple and intuitive model to capture these shapes in the front end of the yield curve when the ELB is binding. We then will use the model to extract the market's expectations about the future monetary policy stance. For now, we ignore the difference between the deposit rate and the short end of the yield curve, and we will discuss how we treat this difference in Section 4. We model the risk-neutral $\mathbb{Q}$ dynamics of the deposit rate, and use it to capture the three shapes of the yield curve in Figure 2.

First, we summarize some basic data features in Figure 3: (1) the deposit rate is discrete and $r_t^d \in \{0, -0.1, -0.2, -0.3, -0.4, ...\}$ percentage point, and (2) the policy rate either stays where it was or moves down by 0.1%, which we formalize as follows[1]:

$$\begin{cases} \mathbb{Q}_t(r_{t+1}^d = r_t^d - 0.1) = \alpha_{1,t}^{\mathbb{Q}} \\ \mathbb{Q}_t(r_{t+1}^d = r_t^d) = 1 - \alpha_{1,t}^{\mathbb{Q}} \end{cases} . \tag{2.1}$$

The simplest model with $\alpha_{1,t}^{\mathbb{Q}} = \alpha_1^{\mathbb{Q}}$ implies one shape of yield curve. See the left panel of Figure 4. This model is a slightly more flexible version of the existing model (see Wu and Xia (2016)), which imposes the restriction $\alpha_1^{\mathbb{Q}} = 0$. However, it cannot capture the rich

[1]In the data, we do not observe the deposit rate move up. For a possible way to incorporate future upward movements, see Wu and Xia (2017).

Figure 3: Deposit rate

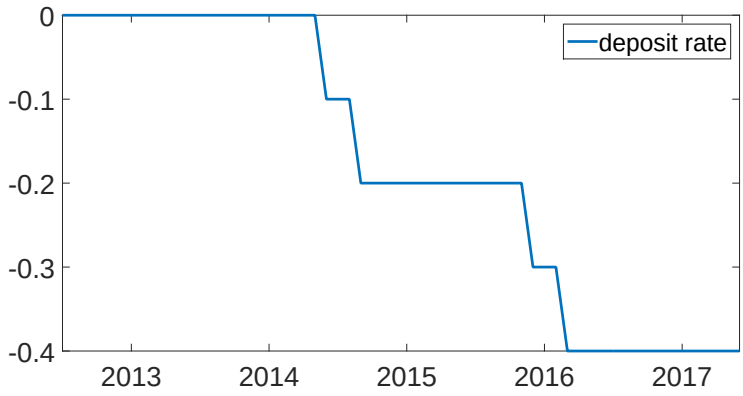

Notes: Sample spans from July 2012 to June 2017.

dynamics in the data in Figure 2. In particular, it cannot capture both a flat curve (left panel) and a downward sloping curve (middle and right panels).

To separate these two shapes, we introduce a binary variable Δ_t, which captures agents' forecast of ECB's next move. $\Delta_t = 1$ indicates a high probability of a cut next period, whereas $\Delta_t = 0$ implies monetary policy is more likely to stay put. We augment (2.1) with Δ_t:

$$\mathbb{Q}_t(r^d_{t+1} = r^d_t - 0.1) = \mathbb{Q}(r^d_{t+1} = r^d_t - 0.1 | r^d_t, \Delta_t) = \alpha^{\mathbb{Q}}_{1,\Delta_t}, \tag{2.2}$$

and $\alpha^{\mathbb{Q}}_{1,\Delta_t=1} > \alpha^{\mathbb{Q}}_{1,\Delta_t=0}$ grants the interpretation of Δ_t.

We model the dynamics of Δ_t as a two-state Markov chain process:

$$\begin{cases} \mathbb{Q}_t(\Delta_{t+1} = 0 | \Delta_t = 0) = \alpha^{\mathbb{Q}}_{00,t} \\ \mathbb{Q}_t(\Delta_{t+1} = 1 | \Delta_t = 1) = \alpha^{\mathbb{Q}}_{11,t} \end{cases}. \tag{2.3}$$

If these probabilities are time invariant, that is, $\alpha^{\mathbb{Q}}_{00,t} = \alpha^{\mathbb{Q}}_{00}$, $\alpha^{\mathbb{Q}}_{11,t} = \alpha^{\mathbb{Q}}_{11}$, this model implies two different shapes for the yield curve: one for $\Delta_t = 1$ and one for $\Delta_t = 0$. The middle panel of Figure 4 provides an example of the two shapes. The blue line captures

Figure 4: Expected paths of the deposit rate

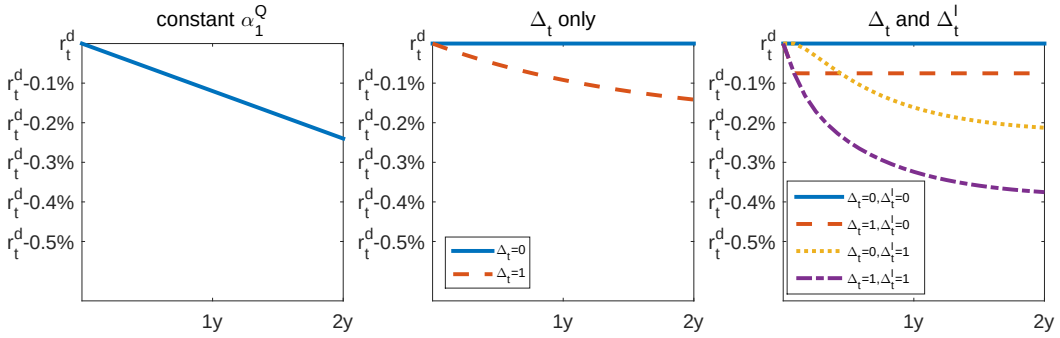

Notes: The chart plots expected paths of deposit rate $\mathbb{E}_t^{\mathbb{Q}}(r_{t+h}^d|\Delta_t, \Delta_t^l, r_t^d)$. The left panel corresponds to the case in which the transition probability for r_t^d is a constant: $\alpha_1^{\mathbb{Q}} = 0.1$. The middle panel corresponds to the case in which the transition probability for r_t^d depends on Δ_t: $\alpha_{1,\Delta_t=0}^{\mathbb{Q}} = 0, \alpha_{1,\Delta_t=1}^{\mathbb{Q}} = 0.1$, and the constant transition probabilities for Δ_t are $\alpha_{00}^{\mathbb{Q}} = 1; \alpha_{11}^{\mathbb{Q}} = 0.95$. The right panel corresponds to the case in which the dynamics of r_t^d depends on both Δ_t and Δ_t^l. The parameters taken from the estimates in Table 1: $\alpha_{1,\Delta_t=0}^{\mathbb{Q}} = 0; \alpha_{1,\Delta_t=1}^{\mathbb{Q}} = 0.75; \alpha_{00,\Delta_t^l=0}^{\mathbb{Q}} = 1; \alpha_{00,\Delta_t^l=1}^{\mathbb{Q}} = 0.82; \alpha_{11,\Delta_t^l=0}^{\mathbb{Q}} = 0.0012; \alpha_{11,\Delta_t^l=1}^{\mathbb{Q}} = 0.75; \alpha_{00}^{l,\mathbb{Q}} = 1; \alpha_{11}^{l,\mathbb{Q}} = 0.88$.

that the yield curve in the state $\Delta_t = 0$ is flat, which corresponds to a long period of time in the data during which the short end of the yield curve is flat, such as the left panel of Figure 2. The red dashed line is for the state $\Delta_t = 1$, which sees a non-negligible probability of the deposit rate moving down. This can explain the shape in the middle panel of Figure 2. However, this model cannot capture the shape in the bottom panel of Figure 2. In this plot, the market expects no immediate cut, but does expect a higher probability of cuts in future meetings.

To accommodate this feature, we devise a separation between the immediate monetary policy stance Δ_t and the longer-term monetary policy stance Δ_t^l. $\Delta_t^l = 1$ implies an easier monetary policy in longer horizons, whereas $\Delta_t^l = 0$ implies a lower possibility for future cuts. We introduce this channel by allowing the dynamics of the state variable Δ_t to depend on Δ_t^l, and (2.3) becomes

$$\begin{cases} \mathbb{Q}_t(\Delta_{t+1} = 0|\Delta_t = 0) = \mathbb{Q}(\Delta_{t+1} = 0|\Delta_t = 0, \Delta_t^l) = \alpha_{00,\Delta_t^l}^{\mathbb{Q}} \\ \mathbb{Q}_t(\Delta_{t+1} = 1|\Delta_t = 1) = \mathbb{Q}(\Delta_{t+1} = 1|\Delta_t = 1, \Delta_t^l) = \alpha_{11,\Delta_t^l}^{\mathbb{Q}} \end{cases} . \tag{2.4}$$

We impose the identification restriction that $\alpha^{\mathbb{Q}}_{00,\Delta^l_t=0} > \alpha^{\mathbb{Q}}_{00,\Delta^l_t=1}$, and the basic intuition is if the economy is currently at the $\Delta_t = 0$ state meaning no immediate cut, the probability of a future cut for $\Delta^l_t = 0$ is less than for $\Delta^l_t = 1$. We further assume

$$\begin{cases} \mathbb{Q}(\Delta^l_{t+1} = 0 | \Delta^l_t = 0) = \alpha^{l,\mathbb{Q}}_{00} \\ \mathbb{Q}(\Delta^l_{t+1} = 1 | \Delta^l_t = 1) = \alpha^{l,\mathbb{Q}}_{11} \end{cases}. \tag{2.5}$$

Our final model, constituting (2.2), (2.4), and (2.5), can capture various shapes of the yield curve; see the right panel of Figure 4. $\Delta_t = 1$ corresponds to the case in which the market highly expects a cut in the next period (see the red dashed line and purple dash-dotted line), whereas $\Delta_t = 0$ corresponds to no immediate cut in the coming month (see the blue solid line and yellow dotted line). $\Delta^l_t = 1$ implies the market expects cuts not necessarily immediately but in the future (see the yellow dotted and purple dash-dotted lines). When $\Delta^l_t = 0$, agents do not anticipate much further cuts past the next month (see blue solid and red dashed lines). The combination of $\Delta_t = 0$ and $\Delta^l_t = 1$ mimics the shape in the right panel of Figure 2.

3 A new shadow rate term structure model

This section incorporates the dynamics for the deposit rate introduced in Subsection 2.2 to an SRTSM. Following Black (1995), the short-term interest rate r_t is the maximum function of the shadow rate s_t and a lower bound. The innovation of our paper is that the lower bound is time varying:

$$r_t = \max(s_t, \underline{r}_t). \tag{3.1}$$

Next, we describe how to model the lower bound and shadow rate, and then discuss bond prices.

3.1 Deposit rate and lower bound

The deposit rate is by definition the lower bound of the Euro OverNight Index Average (EONIA), and hence it naturally serves as the lower bound of the Overnight Index Swap (OIS) curve based on EONIA. We use a discrete-time model with month-end observations as in much of the term structure literature.[2] However, central banks do not meet at the end of the month. For our ELB sample, the ECB meets 8 to 12 times a year, at most once a month, and the meeting dates range from the 1^{st} to the 27^{th} day of the month.

We incorporate this calendar effect when we model the lower bound. Suppose the number of days between the end of current month t and the next meeting date is a fraction γ_t of the month from t to $t+1$. When the ELB is binding, the monthly lower bound $\underline{r}_t$ is the average of the overnight deposit rate for the month:

$$\begin{aligned} \underline{r}_t &\approx \gamma_t r_t^d + (1-\gamma_t)\mathbb{E}_t^{\mathbb{Q}}(r_{t+1}^d) \\ &= r_t^d - (1-\gamma_t)\alpha_{1,\Delta_t} \times 0.1. \end{aligned} \tag{3.2}$$

Note we only align the ECB's meeting schedule with our monthly data for the current month, that is, as of time t,

$$\underline{r}_{t+n} = r_{t+n}^d. \tag{3.3}$$

We assume $\underline{r}_t = 0$ if the economy is not at the ELB.

3.2 Shadow rate and factors

The shadow rate is an affine function of the latent yield factors, often labeled as "level," "slope," and "curvature":

$$s_t = \delta_0 + \delta_1' X_t,$$

[2]For example, see Hamilton and Wu (2012b), Bauer et al. (2012), and Wright (2011).

whose physical dynamics follow a first-order vector autoregression:

$$X_t = \mu + \rho X_{t-1} + \Sigma\varepsilon_t,\ \varepsilon_t \sim N(0, I). \tag{3.4}$$

Similarly, the risk-neutral $\mathbb{Q}$ dynamics are

$$X_t \ = \ \mu^{\mathbb{Q}} + \rho^{\mathbb{Q}} X_{t-1} + \Sigma\varepsilon_t^{\mathbb{Q}},\ \varepsilon_t^{\mathbb{Q}} \sim N(0, I).$$

3.3 Bond prices

The no-arbitrage condition specifies that prices for zero-coupon bonds with different maturities are related by

$$P_{nt} \ = \ \mathbb{E}_t^{\mathbb{Q}} \left[\exp(-r_t) P_{n-1,t+1}\right].$$

The n-period yield relates to the price of the same asset as follows:

$$y_{nt} \ = \ -\frac{1}{n}\log(P_{nt}).$$

Following Wu and Xia (2016), we model forward rates rather than yields for the simplicity of the pricing formula. Define the one-period forward rate f_{nt} with maturity n as the return of carrying a government bond from $t+n$ to $t+n+1$ quoted at time t, which is a simple linear function of yields:

$$f_{nt} \ = \ (n+1)y_{n+1,t} - n y_{nt}.$$

Therefore, modeling forward rates is equivalent to modeling yields. Note that $f_{0t} = y_{1t} = r_t$.

3.3.1 Forward rates with a constant lower bound

If the lower bound were a constant $\underline{r}$, Wu and Xia (2016) show the forward rate can be approximated by

$$f_{nt} \approx \underline{r} + \sigma_n^{\mathbb{Q}} g\left(\frac{a_n + b_n' X_t - \underline{r}}{\sigma_n^{\mathbb{Q}}}\right), \tag{3.5}$$

where the function

$$g(z) = z\Phi(z) + \phi(z). \tag{3.6}$$

Inside the g function, $a_n + b_n' X_t$ is the n-period forward rate from the GATSM. The coefficients a_n and b_n follow a set of difference equations whose solutions are

$$\begin{aligned} a_n &= \delta_0 + \delta_1' \left(\sum_{j=0}^{n-1} \left(\rho^{\mathbb{Q}}\right)^j\right) \mu^{\mathbb{Q}} - \frac{1}{2}\delta_1' \left(\sum_{j=0}^{n-1} \left(\rho^{\mathbb{Q}}\right)^j\right) \Sigma\Sigma' \left(\sum_{j=0}^{n-1} \left(\rho^{\mathbb{Q}}\right)^j\right)' \delta_1 \\ b_n' &= \delta_1' \left(\rho^{\mathbb{Q}}\right)^n. \end{aligned}$$

In addition, $(\sigma_n^{\mathbb{Q}})^2 \equiv \mathbb{V}_t^{\mathbb{Q}}(s_{t+n})$ is the conditional variance of the future shadow rate, and

$$(\sigma_n^{\mathbb{Q}})^2 = \sum_{j=0}^{n-1} \delta_1' (\rho^{\mathbb{Q}})^j \Sigma\Sigma' (\rho^{\mathbb{Q}\prime})^j \delta_1.$$

3.4 Forward rates in the new model

Next, we derive the pricing formula in our new model. We begin by describing the distribution of the lower bound.

3.4.1 Marginal distribution of the lower bound

The probability distribution of interest for pricing purposes is the risk-neutral probability distribution of the lower bound n periods into the future $\mathbb{Q}_t(\underline{r}_{t+n})$. It can be written as the

sum of the joint distributions of the lower bound and Δ, Δ^l states:

$$\mathbb{Q}_t(\underline{r}_{t+n}) = \sum_{\Delta_{t+n},\Delta^l_{t+n}} \mathbb{Q}_t(\underline{r}_{t+n}, \Delta_{t+n}, \Delta^l_{t+n}), \tag{3.7}$$

and the right-hand side has the following dynamics:

$$\begin{aligned}\mathbb{Q}_t(\underline{r}_{t+n}, \Delta_{t+n}, \Delta^l_{t+n}) \quad = \quad & \sum_{\underline{r}^d_{t+n-1},\Delta_{t+n-1},\Delta^l_{t+n-1}} \mathbb{Q}_t(\underline{r}_{t+n-1}, \Delta_{t+n-1}, \Delta^l_{t+n-1}) \\ & \times \mathbb{Q}_t(\underline{r}_{t+n}, \Delta_{t+n}, \Delta^l_{t+n} | \underline{r}_{t+n-1}, \Delta_{t+n-1}, \Delta^l_{t+n-1}),\end{aligned} \tag{3.8}$$

where the transition probability can be decomposed as follows

$$\begin{aligned} & \mathbb{Q}_t(\underline{r}_{t+n}, \Delta_{t+n}, \Delta^l_{t+n} | \underline{r}_{t+n-1}, \Delta_{t+n-1}, \Delta^l_{t+n-1}) \\ = \quad & \mathbb{Q}_t(\underline{r}_{t+n} | \Delta_{t+n}, \Delta^l_{t+n}, \underline{r}_{t+n-1}, \Delta_{t+n-1}, \Delta^l_{t+n-1}) \\ & \times \mathbb{Q}_t(\Delta_{t+n} | \Delta^l_{t+n}, \underline{r}_{t+n-1}, \Delta_{t+n-1}, \Delta^l_{t+n-1}) \\ & \times \mathbb{Q}_t(\Delta^l_{t+n} | \underline{r}_{t+n-1}, \Delta_{t+n-1}, \Delta^l_{t+n-1}) \\ = \quad & \mathbb{Q}(\underline{r}_{t+n} | \underline{r}_{t+n-1}, \Delta_{t+n-1}) \mathbb{Q}(\Delta_{t+n} | \Delta_{t+n-1}, \Delta^l_{t+n-1}) \mathbb{Q}(\Delta^l_{t+n} | \Delta^l_{t+n-1}). \end{aligned} \tag{3.9}$$

The last equal sign is based on the assumptions in (2.2), (2.4), and (2.5), and the assumption that no covariances exist between the three variables. The three terms in (3.9) are specified in (2.2), (2.4), and (2.5).

3.4.2 Pricing formula

With the results in Section 3.4.1, the pricing formula in (3.5) becomes

$$f_{nt} \quad \approx \quad \sum_{\underline{r}_{t+n}} \left(\underline{r}_{t+n} + \sigma^{\mathbb{Q}}_n g \left(\frac{a_n + b_n' X_t - \underline{r}_{t+n}}{\sigma^{\mathbb{Q}}_n} \right) \right) \mathbb{Q}_t(\underline{r}_{t+n}), \tag{3.10}$$

where $\mathbb{Q}(\underline{r}_{t+n})$ is specified in (3.7). Derivations are in Appendix A.1.

The forward rate in (3.10) differs from (3.5) due to the time-varying lower bound. The new pricing formula (3.10) prices in the uncertainty associated with the future dynamics of the lower bound. The forward rate is calculated as an average of forward rates with known $\underline{r}_{t+n}$, weighted by the risk-neutral probability distribution of $\underline{r}_{t+n}$. If $\underline{r}_{t+n}$ were a constant, (3.10) would become (3.5).

The regime-switching dynamics of $(r_t^d, \Delta_t, \Delta_t^l)$ preserve the analytical approximation for the pricing formula. Having an analytical approximation is crucial for the model to be tractable and have better numerical behavior. Dynamic term structure models are often criticized for being difficult to estimate. For example, in the class of GATSM, which is a special case of our model when $\underline{r}_t \to -\infty$ and has analytical bond prices, a literature has been dedicated to improving the model's performance: See Joslin et al. (2011), Christensen et al. (2011), Hamilton and Wu (2012b), Adrian et al. (2012), Creal and Wu (2015), and de Los Rios (2015). If we had to compute bond prices numerically, the model would behave worse.

4 Estimation

4.1 Data and estimation details

Data We model OIS rates on EONIA with data obtained from Bloomberg. Our sample is monthly from July 2005 to June 2017. We date the ELB period when the deposit rate is zero and below starting from July 2012.

Spread The deposit rate is the floor for EONIA. In our model, they are the same for the ELB sample. However, in the data, the former is always lower than the latter. To capture this difference, we introduce a spread. The deposit rate is measured overnight. However, the overnight EONIA rate is very volatile due to some month-end effects. Therefore, we define the spread as the difference between the one-week EONIA rate and overnight deposit rate:

$sp_t = r_t^{week} - r_t^d$. Figure 5 plots the time-series dynamics of the one-week EONIA rate and the overnight deposit rate in the top panel and their difference at the bottom to demonstrate a non-zero and time-varying spread.

Figure 5: Spread

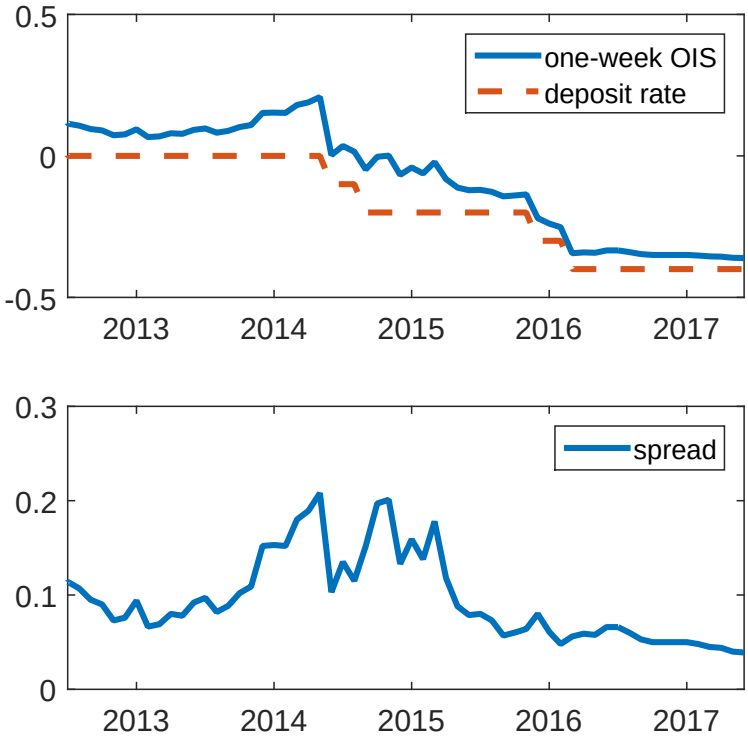

Notes: Top panel: time-series dynamics of the one-week OIS rate in blue solid line and deposit rate in red dashed line; bottom panel: the spread defined as the difference between the two lines in the top panel. X-axis: time. Y-axis: interest rates in percentage points. Sample spans from July 2012 to June 2017.

We assume the spread sp_t follows an AR(1) under the risk-neutral measure:

$$sp_t \quad = \quad \mu_{sp}^{\mathbb{Q}} + \rho_{sp}^{\mathbb{Q}} sp_{t-1} + e_t^{\mathbb{Q}}, \; e_t^{\mathbb{Q}} \sim N(0, \sigma_{sp}^2). \tag{4.1}$$

This modifies the pricing formula in (3.10) to

$$f_{nt} \quad \approx \quad \sum_{\underline{r}_{t+n}} \mathbb{Q}_t(\underline{r}_{t+n}) \left(\underline{r}_{t+n} + c_n + d_n sp_t + \tilde{\sigma}_n^{\mathbb{Q}} g \left(\frac{a_n + b_n' X_t - \underline{r}_{t+n} - c_n - d_n sp_t}{\tilde{\sigma}_n^{\mathbb{Q}}} \right) \right) \tag{4.2}$$

where $c_n = (\sum_{j=0}^{n-1}(\rho_{sp}^{\mathbb{Q}})^j)\mu_{sp}^{\mathbb{Q}}, d_n = (\rho_{sp}^{\mathbb{Q}})^n, (\tilde{\sigma}_n^{\mathbb{Q}})^2 = (\sigma_n^{\mathbb{Q}})^2 + (\sum_{j=0}^{n-1}(\rho_{sp}^{\mathbb{Q}})^{2j})\sigma_{sp}^2$. See Appendix A.2 for the derivation.

Combine (3.1) and (3.2), and add a spread. For ELB, the short rate follows:

$$r_t = r_t^d - (1-\gamma_t)\alpha_{1,\Delta_t}^{\mathbb{Q}} \times 0.1 + sp_t. \tag{4.3}$$

Forward rates We take OIS yields with the following maturities: three and six months, and one, two, three, five, six, seven, eight, nine, and ten years, and transform them into forward rates. A forward contract carrying a government bond from $t+n$ to $t+n+m$ pays an average interest rate

$$f_{nmt} = \frac{1}{m}(f_{nt} + f_{n+1,t} + ... + f_{n+m-1,t}), \tag{4.4}$$

where f_{nt} is in (4.2). The forward rates we model include $f_{3,3,t}$, $f_{6,6,t}$, $f_{12,12,t}$, $f_{24,12,t}$, $f_{60,12,t}$, $f_{84,12,t}$, and $f_{108,12,t}$.

There are a couple of advantages of modeling forwards rates over yields. First, forward rates require summing over fewer terms per (4.4). Second, forward rates do not involve the "max" operator, which will be included in yields of any maturity. Having the "max" operator is problematic for any gradient-based numerical optimizer.

State space form The state variables X_t, Δ_t, and Δ_t^l are latent, whereas r_t^d and sp_t are observed. Our SRTSM is a nonlinear state-space model. The transition equations include (3.4), and the $\mathbb{P}$ version of (2.2), (2.4), (2.5), and (4.1), where we assume the same process under the physics dynamics $\mathbb{P}$ and risk-neutral dynamics $\mathbb{Q}$ but with different parameters. The difference between them captures the risk premium.

Adding measurement errors to (4.3) and (4.4), the measurement equations are

$$r_t^o = r_t + \eta_t \tag{4.5}$$

$$f_{nmt}^o = f_{nmt} + \eta_{nmt}, \tag{4.6}$$

where "o" superscript stands for observation, and the measurement errors are i.i.d. normal: $\eta_t, \eta_{nmt} \sim N(0, \omega^2)$.

Normalization The collection of parameters we estimate consists of four subsets: (1) parameters related to r_t^d, Δ_t, ssand Δ_t^l, including $\alpha_{1,\Delta_t=0}$, $\alpha_{1,\Delta_t=1}$, $\alpha_{00,\Delta_t^l=0}$, $\alpha_{11,\Delta_t^l=0}$, $\alpha_{00,\Delta_t^l=1}$, $\alpha_{11,\Delta_t^l=1}$, α_{00}^l, α_{11}^l and $\alpha_{1,\Delta_t=0}^{\mathbb{Q}}$, $\alpha_{1,\Delta_t=1}^{\mathbb{Q}}$, $\alpha_{00,\Delta_t^l=0}^{\mathbb{Q}}$, $\alpha_{11,\Delta_t^l=0}^{\mathbb{Q}}$, $\alpha_{00,\Delta_t^l=1}^{\mathbb{Q}}$, $\alpha_{11,\Delta_t^l=1}^{\mathbb{Q}}$, $\alpha_{00}^{l,\mathbb{Q}}$, $\alpha_{11}^{l,\mathbb{Q}}$. (2) parameters describing the dynamics of sp_t, including $(\mu_{sp}, \mu_{sp}^{\mathbb{Q}}, \rho_{sp}, \rho_{sp}^{\mathbb{Q}}, \sigma_{sp})$; (3) parameters related to X_t, including $(\mu, \mu^{\mathbb{Q}}, \rho, \rho^{\mathbb{Q}}, \Sigma, \delta_0, \delta_1)$; and (4) the parameter for pricing error: ω. For identification, we impose $\alpha_{1,\Delta_t=1}^{\mathbb{Q}} > \alpha_{1,\Delta_t=0}^{\mathbb{Q}}$ and $\alpha_{00,\Delta_t^l=0}^{\mathbb{Q}} > \alpha_{00,\Delta_t^l=1}^{\mathbb{Q}}$. The identifying restrictions on the group (3) are similar to Hamilton and Wu (2014): (i) $\delta_1 = [1,1,1]'$, (ii)$\mu^{\mathbb{Q}} = 0$, (iii) $\rho^{\mathbb{Q}}$ is diagonal with eigenvalues in descending order, and (iv) Σ is lower triangular.

Estimation We estimate the model by maximum likelihood using the algorithm for regime-switching state space models of Kim (1994). In practice, we impose $r_t^d \in \{0, -0.1, -0.2, -0.3, -0.4, ..., -1\}$, and therefore $\mathbb{Q}(r_{t+1}^d = r_t^d - 0.1 | r_t^d = -1, \Delta_t) = 0$.

We report maximum likelihood estimates and robust standard errors (see Hamilton (1994)) in Table 1. The eigenvalues of ρ, $\rho^{\mathbb{Q}}$ indicate the factors X_t are highly persistent under both measures. This finding is consistent with the term structure literature. Both $\alpha_{1,\Delta_t=0}$ and $\alpha_{1,\Delta_t=0}^{\mathbb{Q}}$ are zero, which means that when $\Delta_t = 0$, agents do not expect the deposit rate to change in the next period. When $\Delta_t = 1$, the probability of the ECB cutting the deposit rate is much higher: $\alpha_{1,\Delta_t=1} = 1$ under the physical measure, and $\alpha_{1,\Delta_t=1}^{\mathbb{Q}} = 0.75$ under the risk-neutral measure. The difference between the two measures reflects the risk

Table 1: Maximum likelihood estimates

$\alpha_{1,\Delta_t=0}$	0.0000			$\alpha^{\mathbb{Q}}_{1,\Delta_t=0}$	0.0000		
	(0.0000)				(0.0000)		
$\alpha_{1,\Delta_t=1}$	1.0000			$\alpha^{\mathbb{Q}}_{1,\Delta_t=1}$	0.7510		
	(0.0000)				(0.1777)		
$\alpha_{00,\Delta^l_t=0}$	0.9464			$\alpha^{\mathbb{Q}}_{00,\Delta^l_t=0}$	1.0000		
	(0.0344)				(0.0000)		
$\alpha_{11,\Delta^l_t=0}$	0.0002			$\alpha^{\mathbb{Q}}_{11,\Delta^l_t=0}$	0.0012		
	(0.0005)				(0.0023)		
$\alpha_{00,\Delta^l_t=1}$	0.8857			$\alpha^{\mathbb{Q}}_{00,\Delta^l_t=1}$	0.8232		
	(0.0770)				(0.0587)		
$\alpha_{11,\Delta^l_t=1}$	0.0000			$\alpha^{\mathbb{Q}}_{11,\Delta^l_t=1}$	0.7516		
	(0.0001)				(0.1726)		
α^l_{00}	0.9735			$\alpha^{l,\mathbb{Q}}_{00}$	1.0000		
	(0.0265)				(0.0000)		
α^l_{11}	0.9013			$\alpha^{l,\mathbb{Q}}_{11}$	0.8815		
	(0.0331)				(0.0429)		
$1200\mu_{sp}$	0.0114			$1200\mu^{\mathbb{Q}}_{sp}$	0.0084		
	(0.0000)				(0.0049)		
ρ_{sp}	0.8674			$\rho^{\mathbb{Q}}_{sp}$	0.9361		
	(0.0000)				(0.0407)		
$1200\sigma_{sp}$	0.0786						
	(0.0045)						
1200μ	-0.0272	-1.2246	0.9167	$1200\mu^{\mathbb{Q}}$	0	0	0
	(0.1385)	(1.2907)	(1.2592)				
ρ	0.9932	0.0265	0.0228	$\rho^{\mathbb{Q}}$	0.9964	0	0
	(0.0250)	(0.0177)	(0.0181)		(0.0005)		
	-0.1136	0.4675	-0.4494		0	0.9293	0
	(0.2628)	(1.3064)	(1.3295)			(0.0032)	
	0.0581	0.3983	1.3133		0	0	0.9257
	(0.2547)	(1.2818)	(1.3047)				(0.0034)
$\lvert eig(\rho)\rvert$	0.9875	0.8939	0.8939				
δ_0	7.6098						
	(0.5368)						
1200Σ	0.5961	0	0				
	(0.0511)						
	-12.5099	10.4538	0				
	(0.8773)	(0.2589)					
	11.8193	-10.3705	0.1715				
	(0.8712)	(0.2415)	(0.0264)				
1200ω	0.0235						
	(0.0000)						

Notes: Maximum likelihood estimates with quasi-maximum likelihood standard errors in parentheses. Sample: July 2005 to June 2017.

Figure 6: Filtered probabilities for different states

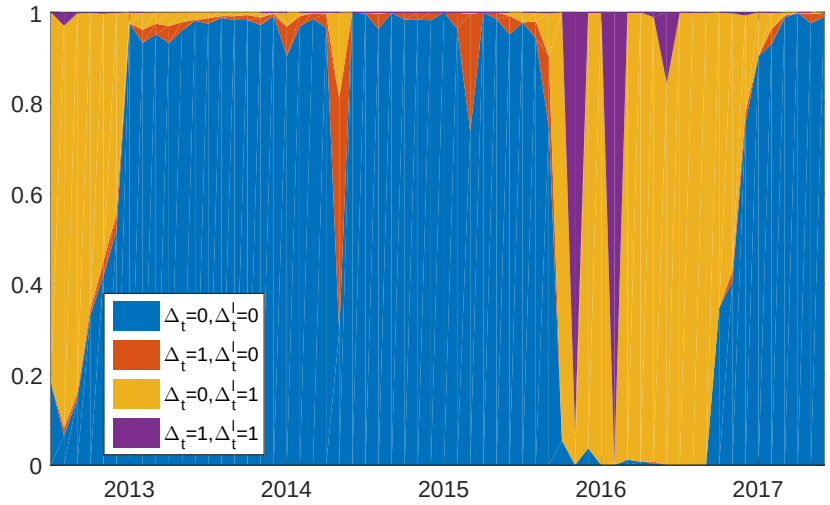

Notes: Areas with different colors correspond to the filtered probabilities of different states. From the bottom to top are: blue for $\Delta_t = 0, \Delta_t^l = 0$, red for $\Delta_t = 1, \Delta_t^l = 0$, yellow for $\Delta_t = 0, \Delta_t^l = 1$, and purple for $\Delta_t = 1, \Delta_t^l = 1$.

premium. The $\Delta_t = 0$ state is very persistent, with the probability of staying in this state (α_{00,Δ_t^l}, $\alpha^{\mathbb{Q}}_{00,\Delta_t^l}$) being 95% or 100% for $\Delta_t^l = 0$, and 89% or 82% for $\Delta_t^l = 1$. By contrast, the $\Delta_t = 1$ state is much less persistent. The spread sp_t follows a persistent autoregressive process under both measures. Other parameters controlling level and scale are comparable to what we see in the literature.

4.2 Filtered probabilities

Figure 6 plots the filtered probabilities for each state. Blue is the dominant state: it covers most of the space from December 2012 to September 2015 and from December 2016 to the end of the sample, which constitutes 70% of the ELB period. In this state, the yield curve is basically flat (see the blue line in the right panel of Figure 4). The remaining of the sample are mainly in yellow and purple. The probability of the purple state peaked twice in November 2015 and February 2016, which are the months before the ECB lowered the deposit rate to -0.3% and -0.4%, respecivley. The purple area corresponds to the purple line

in the right panel of Figure 4, and the yield curve is downward sloping. The yellow state corresponds to the yellow line in Figure 4, where the yield curve is initially flat, and then trend downwards. This means agents do not expect the central bank to cut rates in the next month. However, they do expect future actions. The yellow area dominates between July and November in 2012, and from March to November in 2016. The least prominent state is in red, which implies agents expect the central bank to make an immediate cut, but they also think this cut is the last one in the history. This scenario appears less plausible.

5 NIRP and the yield curve

5.1 Extracting the market's expectations on the NIRP from the yield curve

Figure 7: Probability of rate cut

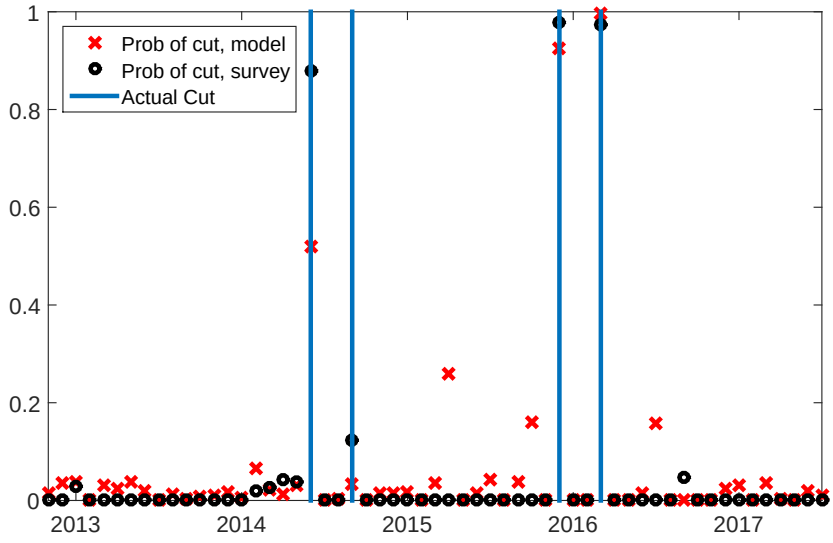

Notes: Red crosses: time $t-1$ probability of rate cut for month t from our model: $\mathbb{P}_{t-1}(r_t^d = r_{t-1}^d - 0.1) = \alpha_{1,\Delta_{t-1}=0} \times \mathbb{P}_{t-1}(\Delta_{t-1} = 0) + \alpha_{1,\Delta_{t-1}=1} \times \mathbb{P}_{t-1}(\Delta_{t-1} = 1)$. Black circles: Bloomberg survey expectation, measured as the fraction of respondents that expect a cut. Blue bars: the four rate cuts in June 2014, September 2014, December 2015, and March 2016. X-axis: time. Y-axis: probability.

In this section, we extract market expectations of the NIRP from our SRTSM. Figure 7 plots the four actual cuts in blue vertical bars together with our model predictions in red crosses and Bloomberg survey expectations in black dots. On June 5, 2014, the ECB cuts the rate from 0 to -0.1% for the first time. In May, our model predicts this event with more than 50% probability. As a comparison, over 90% of the respondents of the Blomberg survey expected the cut. The second cut in September 2014 was a surprise to both economists and the market. The next two cuts from -0.2% to -0.3%, and then subsequently to -0.4%, were largely anticipated. For the rest of the meetings, market participants do not price in much probability of an immediate cut. This exercise confirms market participants' expectations are consistent with economists' view.

Figure 8: Expected deposit facility rate

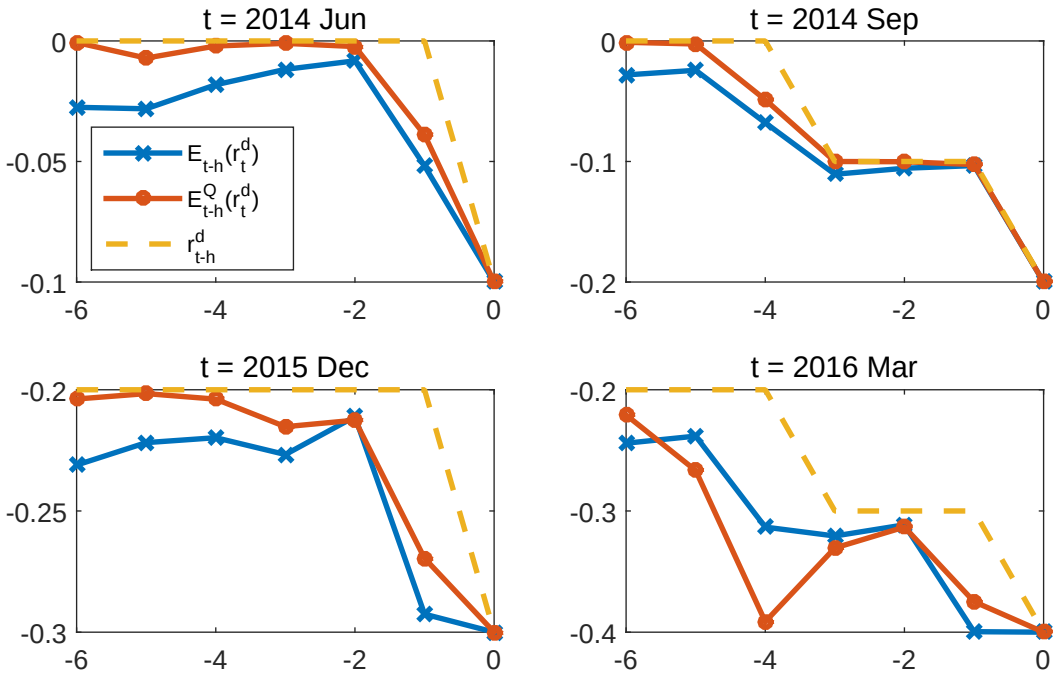

Notes: Blue lines with crosses are $\mathbb{E}_{t-h}(r_t^d)$; red lines with dots are $\mathbb{E}^{\mathbb{Q}}_{t-h}(r_t^d)$; yellow dashed lines are r^d_{t-h}. t = June 2014 (top left), September 2014 (top right), December 2015 (bottom left), and March 2016 (bottom right). X-axis: $-h$, Y-axis: annualized interest rates in percentage points.

The Bloomberg survey is conducted one week before the meeting. The yield curve,

however, contains richer information and further into the future. In Figure 9, we further inspect for how long the market has anticipated some of the developments. It plots the market's expectations h months before the four event dates for $h = 0, 1, 2, ..., 6$. The blue lines with crosses are the physical expectations $\mathbb{E}_{t-h}(r_t^d)$, the red lines with dots are the risk-neutral expectations $\mathbb{E}_{t-h}^{\mathbb{Q}}(r_t^d)$, and the then deposit rates r_{t-h}^d are in yellow dashed lines. The difference between the yellow and the other colors capture an expected future cut. The difference between the blue and red lines captures the risk premium.

Consistent with Figure 7, the June 2014 and December 2015 cuts were anticipated one month ahead, whereas the September 2014 cut was completely unanticipated. The most interesting case is March 2016. A cut to -0.35% was expected 4 months before, when the actual rate was -0.2% under the risk-neutral expectation. Then agents revised up their expectations for the next two months. Eventually, when $h = 1$, agents fully priced in the -0.4% for the next month.

5.2 Policy counterfactual analyses

Much of the existing literature has focused on whether and how much negative interest rate policy has affected banks' profitability; see, for example, Borio et al. (2015), Jobst and Lin (2016), and Cœuré (2016). Our paper evaluates this policy's impact on the yield curve, which links financial markets and the macroeconomy.

We perform the following experiment: suppose the central bank could make commitments to change Δ_t, and/or Δ_t^l, what would happen to the yield curve? We conduct this exercise at the end of our sample in June 2017, which, according to Figure 6, has a probability of 99% in the blue state $\Delta_t = 0, \Delta_t^l = 0$, where agents expect the central bank to stay put for both the short run and long run. In our exercise, we assume agents fully internalize the ECB's announcement and deem it fully credible.

First, suppose the ECB indicated an easing position in the next meeting, but promised this cut would be the last one in history. Then the one month rate would decrease by 0.03%

Figure 9: Counterfactual analysis

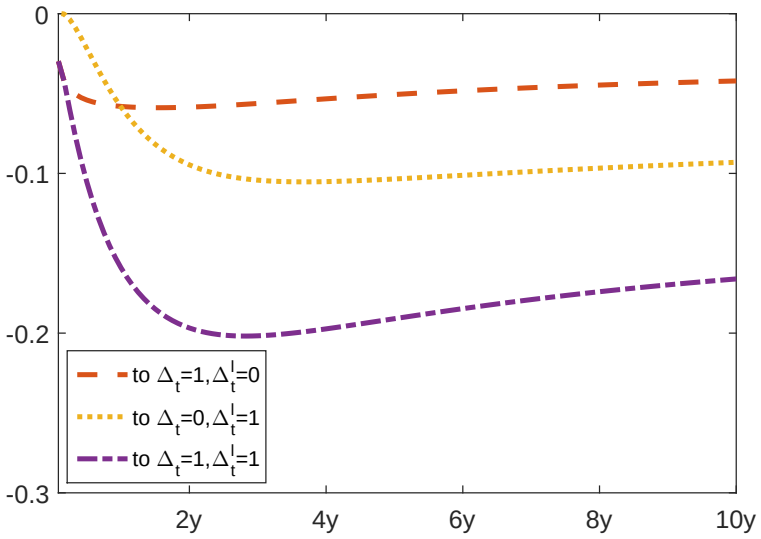

Notes: This chart plots the change of the yield curve as of June 2017 if we change Δ_t, Δ_t^l to $\Delta_t = 1, \Delta_t^l = 0$ in the red dashed line, to $\Delta_t = 0, \Delta_t^l = 1$ in the yellow dotted line, and to $\Delta_t = 1, \Delta_t^l = 1$ in the purple dashed-dotted line.

(see the red dashed line): Δ_t would move from 0 to 1, making the expected deposit rate one month from now 0.075% lower. In addition, the next meeting happens on July 20, which is 0.6 of the month from the end of June to end of July. The current level of the deposit rate would prevail for 60% of the month, and the lower deposit rate would happen for the next 40%. Therefore, $0.075\% \times 0.6 = 0.03\%$. The red curve is almost flat.

Second, if the central bank announced it would not make any move in the next meeting, but the overall future environment would be expansionary, the change in the yield curve would be as in the yellow dotted line. The one month rate would not move, but yields at other maturities would decrease. The change would grow with the maturity up to two years, and then flatten out afterwards at about 0.1%.

Third, suppose the ECB communicated with the public about its expansionary plan across all horizons. Then the change in the yield curve would be as in the purple dashed-dotted line, which would be the largest among all three lines. The initial change would be the same as in the red line. But after one month, the change would be much larger, and the

largest change would happen in about 2 years at 0.2%. Then, it would decrease to about 0.16% in the long run. The NIRP announcement would have less of an impact in the long run, because the chance for the ELB to be binding is smaller.

6 Yield curve implications

6.1 Model comparison

Table 2: Model comparison

		M_{main}	M_{Δ_t}	M_{S-TV}	M_{S-0}	$M_{S-.4}$	M_G
full sample	log likelihood	**935.48**	911.94	709.55	279.12	577.97	603.32
	(n,m)	Measurement errors of f_{nmt}					
	(0,1)	**3.62**	4.11	8.01	14.32	4.08	5.50
	(3,3)	**6.20**	6.51	6.39	16.04	9.66	7.38
	(6,6)	**5.83**	6.66	6.72	16.70	9.92	9.06
	(12,12)	6.24	6.48	6.81	16.21	10.22	**5.91**
	(24,12)	**8.75**	8.92	9.33	15.14	10.75	11.10
	(60,12)	8.25	8.47	**8.24**	9.34	8.38	8.44
	(84,12)	5.05	**4.94**	4.96	6.18	5.36	5.79
	(108,12)	8.17	8.20	**8.13**	9.01	8.67	8.77
ELB	(n,m)	Measurement errors of f_{nmt}					
	(0,1)	1.42	**1.35**	10.67	20.89	3.39	3.98
	(3,3)	**3.64**	3.93	3.97	22.44	11.81	4.41
	(6,6)	**3.87**	4.83	5.08	23.52	12.91	6.56
	(12,12)	3.40	4.38	5.52	22.66	12.52	**1.91**
	(24,12)	**4.59**	4.89	6.67	18.71	10.64	9.69
	(60,12)	8.92	9.17	8.97	11.24	**8.90**	9.16
	(84,12)	**4.32**	4.74	4.81	6.55	4.86	6.82
	(108,12)	**6.92**	7.10	7.39	8.36	7.47	9.29

Notes: Top panel: full sample from July 2005 to June 2017; bottom panel: ELB sample from July 2012 to June 2017. First column: our main model M_{main}; second column: M_{Δ_t} without Δ_t^l; third column: benchmark shadow rate model M_{S-TV} with myopic agents and time-varying lower bound equal to the deposit rate; fourth column: benchmark shadow rate model M_{S-0} with a constant lower bound at zero; fifth column: benchmark shadow rate model $M_{S-.4}$ with a constant lower bound at -0.4%; sixth column: benchmark GATSM. Measurement errors are in basis points, and computed as the root-mean-square errors between observed and model-implied short rates and forward rates. Forward rate f_{nmt} is the forward contract from $t+n$ to $t+n+m$. We highlight the smallest measurement errors, and the highest log likelihood value.

Table 2 compares our model with several alternatives in terms of log likelihood values,

Figure 10: Fitted yield curves

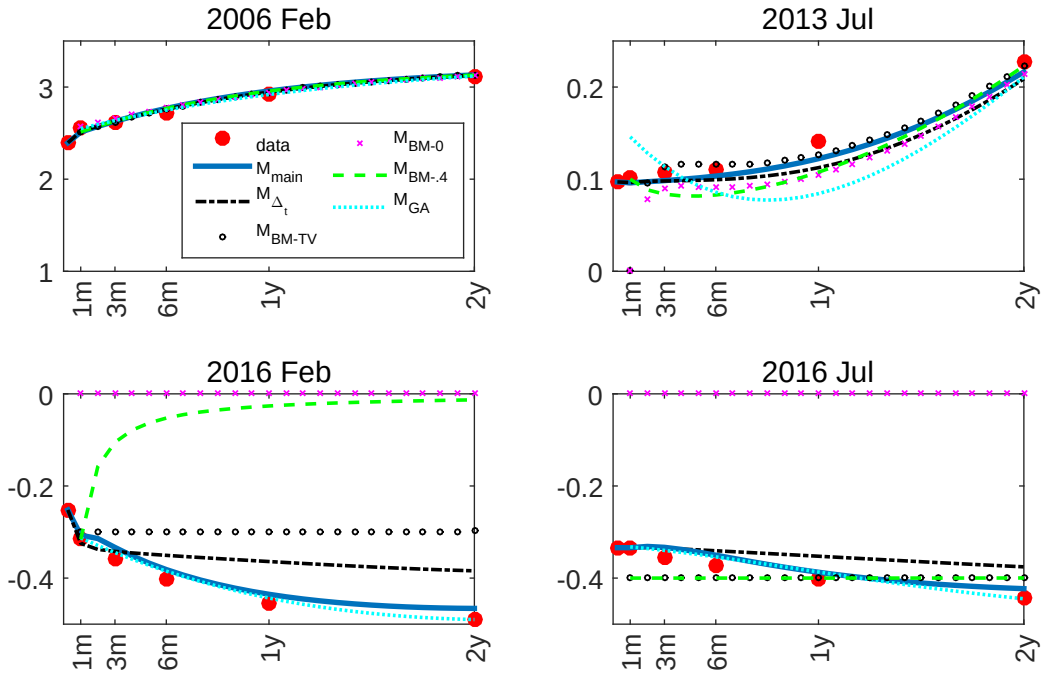

Notes: Red dots: observed data; blue solid line: our main model M_{main}; black dash-dotted line: M_{Δ_t} without Δ_t^l; black circles: benchmark model M_{BM-TV} with exogenously varying lower bound; pink cross: benchmark model M_{BM-0} with a constant lower bound at zero; green dashed line: benchmark model $M_{BM-.4}$ with a constant lower bound at -0.4%; light blue dotted line: GATSM M_G. X-axis: maturity; Y-axis: interest rates in percentage points. Top left panel: February 2006; top right panel: July 2013; bottom left: February 2016; bottom right: July 2016.

information criteria, and measurement errors. The first column is our main model specification. The second columns is our model without Δ_t^l. Columns 3 to 5 are benchmark shadow rate models in the literature, and the corresponding lower bounds are specified as the current deposit rate, 0, and -0.4%, respectively. The last column is the GATSM. See details in Appendix C.

Our main model has the highest likelihood value. Our main model also provides the best overall fit to the forward curve with smaller measurement errors. All the evidence points to the conclusion that the data favor our main model over these alternative model specifications.

Figure 10 provides some visual evidence by comparing the observed data in red dots with various model-implied yield curves. When the ELB was not binding, all models fit the data

similarly well (see the top left panel). When the yield curve has a flat short end at the beginning of the ELB, our main model and M_{Δ_t} provide a better fit than other models (see the top right panel). In theory, the benchmark shadow rate models M_{S-TV}, M_{S-0}, and $M_{S-.4}$ should have similar performance. But in practice, because they ignore the spread between the deposit rate and EONIA, there are discrepancies at the very short end. The GATSM is expected to perform poorly in this case, which is what motivates the entire literature on the SRTSM. Not able to fit the flat short end of the yield curve makes the GATSM one of the worst models; see Table 2.

In the bottom panels, none of the shadow rate models existing in the literature are able to generate a downward sloping short end to mimic the data when the ELB is binding. Intuitively, agents in these models are myopic, and do not expect further development of the policy rate. Both our main model and M_{Δ_t} are able to generate a downward slope through agents' expectations that the future deposit rate might further decrease. However, M_{Δ_t} is not flexible enough to match the data for either February or July 2016. Our main model, which is motivated by various shapes of the yield curve in Figure 2, fits the data well. Although the GATSM is able to fit the downward sloping short end, it does not provide an intuitive interpretation of the market's expectation on the NIRP.

6.2 Term premium

The term premium is one of the focal points for the term structure literature; see, for example, Duffee (2002), Wright (2011), Bauer et al. (2012, 2014), and Creal and Wu (2016). We compute the 10-year yield term premium for the Euro area from our main model, and plot it in the blue solid line in Figure 11.

The term premia have trended down since 2009. At the ELB, we observe some negative term premia. This observation can mainly be attributed to the QE programs, which purchase longer-term government bonds and reduce yields through the term premium channel. For empirical evidence, see Gagnon et al. (2011), Krishnamurthy and Vissing-Jorgensen (2011),

Figure 11: 10-year term premium

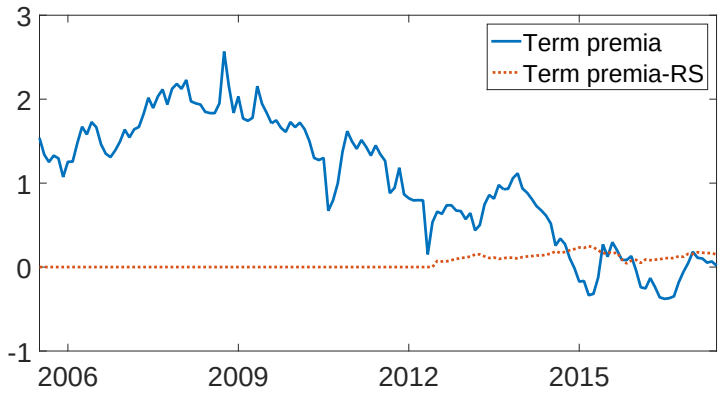

Notes: Blue solid line: 10-year term premium from our main model; red dashed line: the regime-switching portion of term premium. X-axis: time; Y-axis: interest rates in percentage points. Sample spans from July 2005 to June 2017.

and Hamilton and Wu (2012a).

A new question in our context is whether the time variation of the deposit rate incurs an additional term premium on the longer-term yield. To address this question, we plot the portion of the term premium that is due to the dynamics of the deposit rate with the red dotted line in Figure 11. It is positive and in the order of magnitude of 0.1%. This result attributes most of the term premium to uncertainty about the underlying latent factors, because (1) parameters governing the deposit rate do not differ much between the physical and risk-neutral dynamics, and (2) at longer horizons, agents expect the ELB will be lifted, and therefore the long rates do not depend much on how we model the dynamics of the deposit rate.

7 Conclusion

We have proposed a new shadow rate term structure model that captures the NIRP in the Euro area. We model the discrete movement of the deposit rate with a simple and intuitive regime-switching model. To capture the rich dynamics in the short end of the yield curve, we introduce two latent state variables: one captures the immediate monetary policy

stance, and the other captures the future monetary policy stance in longer horizons. We illustrate that the two do not always coincide, and therefore, it is useful to have both of the indicators. Compared to alternative models, including several shadow rate term structure models proposed in the literature, and the Gaussian affine term structure model, our new model fits the data the best.

We use our model to extract the market's expectations on the NIRP. Overall, expectations of financial market participants from our model agree with economists' expectations of the Bloomberg survey. Importantly, our model has the advantage over the Bloomberg survey because we can extract the market's expectations further into the future, whereas the Bloomberg surveys are collected only one week before meetings for monetary policy. We find the June 2014 cut and December 2015 cut were expected the month before, and the September 2014 cut was entirely unanticipated. Most interestingly, the March 2016 cut was expected 4 months before the actual cut.

We then evaluate the NIRP's impact on the yield curve with some counterfactual analyses. We find making the immediate monetary policy expansionary would decrease the one month rate by 0.03% in June 2017. Making no immediate action but promising an expansionary environment in the future would lower the yield curve by 0.1% at the 2 to 10 year horizon. If the central bank could commit to an expansionary policy in both the short and long run, the impact would be the largest, and the two year yield would decrease by 0.2%, and the long term yield would decrease by 0.16%.

The 10-year term premium increased between 2005 and 2008. It has trended down since 2009, with negative numbers at the ELB, potentially due to QE purchases. The dynamics of the deposit rate contributes positively to the premium, but at a smaller order of magnitude.

References

Adrian, Tobias, Richard K. Crump, and Emanuel Moench, "Pricing the term structure with linear regressions.," 2012, *110* (1), 110–138.

Ang, Andrew and Geert Bekaert, "Regime Switches in Interest Rates," *Journal of Business & Economic Statistics*, 2002, *20* (2), 163–182.

Bansal, Ravi and Hao Zhou, "Term structure of interest rates with regime shifts," *The Journal of Finance*, 2002, *57* (5), 1997–2043.

Bauer, Michael D. and Glenn D. Rudebusch, "Monetary Policy Expectations at the Zero Lower Bound," *Journal of Money, Credit and Banking*, 2016, *48* (7), 1439–1465.

_ , _ , and Jing Cynthia Wu, "Correcting Estimation Bias in Dynamic Term Structure Models," *Journal of Business & Economic Statistics*, 2012, *30* (3), 454–467.

_ , _ , and _ , "Term Premia and Inflation Uncertainty: Empirical Evidence from an International Panel Dataset: Comment," *American Economic Review*, January 2014, *104* (1), 323–37.

Black, Fischer, "Interest Rates as Options," *Journal of Finance*, 1995, *50*, 1371–1376.

Borio, Claudio EV, Leonardo Gambacorta, and Boris Hofmann, "The Influence of Monetary Policy on Bank Profitability," 2015. BIS working paper.

Christensen, J. H. E. and Glenn D. Rudebusch, "Estimating shadow-rate term structure models with near-zero yields," *Journal of Financial Econometrics*, 2014, *0*, 1–34.

Christensen, Jens H.E., Francis X. Diebold, and Glenn D. Rudebusch, "The affine arbitrage-free class of Nelson-Siegel term structure models.," 2011, *164* (1), 4–20.

Cœuré, Benoît, "Assessing the implications of negative interest rates," in "speech at the Yale Financial Crisis Forum, Yale School of Management, New Haven," Vol. 28 2016.

Creal, Drew D. and Jing Cynthia Wu, "Estimation of affine term structure models with spanned or unspanned stochastic volatility," *Journal of Econometrics*, 2015, *185* (1), 60 – 81.

_ **and** _ , "Bond risk premia in consumption based models.," 2016. Working paper, University of Chicago, Booth School of Business.

Dai, Qiang, Kenneth J Singleton, and Wei Yang, "Regime shifts in a dynamic term structure model of US treasury bond yields," *Review of Financial Studies*, 2007, *20* (5), 1669–1706.

de Los Rios, Antonio Diez, "A New Linear Estimator for Gaussian Dynamic Term Structure Models," *Journal of Business & Economic Statistics*, 2015, *33* (2), 282–295.

Duffee, Gregory R., "Term premia and interest rate forecasts in affine models," 2002, *57* (1), 405–443.

Gagnon, Joseph, Mattew Raskin, Julie Remache, and Brian Sack, "The Financial Market Effects of the Federal Reserve's Large-Scale Asseet Purchase," *International Journal of Central Banking*, 2011, *7*, 3–43.

Hamilton, James D., "A New Approach to the Economic Analysis of Nonstationary Time Series and the Business Cycle," *Econometrica*, 1989, *57* (2), 357–384.

_ , *Time Series Analysis*, Princeton, New Jersey: Princeton University Press, 1994.

_ **and Jing Cynthia Wu**, "The effectiveness of alternative monetary policy tools in a zero lower bound environment," 2012, *44 (s1)*, 3–46.

_ **and** _ , "Identification and estimation of Gaussian affine term structure models.," 2012, *168* (2), 315–331.

_ **and** _ , "Testable Implications of Affine Term Structure Models," *Journal of Econometrics*, 2014, *178*, 231–242.

Ichiue, Hibiki and Yoichi Ueno, "Estimating Term Premia at the Zero Bound : an Analysis of Japanese, US, and UK Yields," 2013. Bank of Japan Working Paper.

Jobst, Andreas and Huidan Lin, "Negative Interest Rate Policy (NIRP): Implications for Monetary Transmission and Bank Profitability in the Euro Area," 2016. IMF working paper.

Joslin, Scott, Kenneth J. Singleton, and Haoxiang Zhu, "A new perspective on Gaussian affine term structure models," 2011, *27*, 926–970.

Kim, Chang-Jin, "Dynamic linear models with Markov-switching," *Journal of Econometrics*, 1994, *60* (1-2), 1–22.

Kim, Don H. and Kenneth J. Singleton, "Term Structure Models and the Zero Bound: an Empirical Investigation of Japanese Yields," *Journal of Econometrics*, 2012, *170*, 32–49.

Kortela, Tomi, "A shadow rate model with time-varying lower bound of interest rates," 2016. Bank of Finland Research Discussion Paper.

Krippner, Leo, "A Tractable Framework for Zero Lower Bound Gaussian Term Structure Models," August 2013. Australian National University CAMA Working Paper 49/2013.

Krishnamurthy, Arvind and Annette Vissing-Jorgensen, "The Effects of Quantitative Easing on Interest Rates: Channels and Implications for Policy," *Brookings Papers on Economic Activity*, 2011, *2*, 215–265.

Lemke, Wolfgang and Andreea L Vladu, "Below the zero lower bound: A shadow-rate term structure model for the euro area," 2016. Deutsche Bundesbank Discussion Paper.

Renne, Jean-Paul, "A model of the euro-area yield curve with discrete policy rates," *Studies in Nonlinear Dynamics & Econometrics*, 2012.

Wright, J. H., "Term Premia and Inflation Uncertainty: Empirical Evidence from an International Panel Dataset," *American Economic Review*, 2011, *101*, 1514–1534.

Wu, Jing Cynthia and Fan Dora Xia, "Measuring the macroeconomic impact of monetary policy at the zero lower bound.," *Journal of Money, Credit and Banking*, 2016, *48* (2-3), 253–291.

_ **and** _ , "Time-varying lower bound of interest rates in Europe," 2017. Working paper, University of Chicago, Booth School of Business.

Appendix A Deriving pricing formula

As shown in Wu and Xia (2016), the forward rate is

$$f_{nt} \approx \mathbb{E}_t^{\mathbb{Q}}[r_{t+n}] - \frac{1}{2}\left(\mathbb{V}\text{ar}_t^{\mathbb{Q}}\left[\sum_{j=1}^{n} r_{t+j}\right] - \mathbb{V}\text{ar}_t^{\mathbb{Q}}\left[\sum_{j=1}^{n-1} r_{t+j}\right]\right). \tag{A.1}$$

Appendix A.1 Model with $\underline{r}_{t+n}$

Wu and Xia (2016) show (A.1) can be further approximated:

$$f_{nt} \approx \mathbb{E}_t^{\mathbb{Q}}[\max(s_{t+n}, \underline{r}_{t+n})] - \mathbb{Q}_t(s_{t+n} \geq \underline{r}_{t+n}) \times \frac{1}{2}\left(\mathbb{V}\text{ar}_t^{\mathbb{Q}}\left[\sum_{j=1}^{n} s_{t+j}\right] - \mathbb{V}\text{ar}_t^{\mathbb{Q}}\left[\sum_{j=1}^{n-1} s_{t+j}\right]\right).$$

The right-hand side equals

$$\int \left[-\mathbb{Q}_t(s_{t+n} \geq \underline{r}_{t+n}|\underline{r}_{t+n}) \times \frac{1}{2}\left(\mathbb{V}\text{ar}_t^{\mathbb{Q}}\left[\sum_{j=1}^{n} s_{t+j}\right] - \mathbb{V}\text{ar}_t^{\mathbb{Q}}\left[\sum_{j=1}^{n-1} s_{t+j}\right]\right)\right.$$
$$\left. + \mathbb{E}_t^{\mathbb{Q}}[\max(s_{t+n}, \underline{r}_{t+n}|\underline{r}_{t+n})]\right] \mathbb{Q}_t(\underline{r}_{t+n}) d\underline{r}_{t+n}.$$

According to Wu and Xia (2016), the expression inside the integral conditioning on the lower bound equals

$$\underline{r}_{t+n} + \sigma_n^{\mathbb{Q}} g\left(\frac{a_n + b_n' X_t - \underline{r}_{t+n}}{\sigma_n^{\mathbb{Q}}}\right).$$

Hence, we obtain (3.10).

Appendix A.2 Model with $\underline{r}_{t+n}$ and sp_{t+n}

First,

$$\mathbb{Q}_t(s_{t+n} - sp_{t+n}) \sim N\left(\bar{a}_n + b_n' X_t - c_n - d_n sp_t, (\tilde{\sigma}_n^{\mathbb{Q}})^2\right),$$

where $\bar{a}_n \equiv \delta_0 + \delta_1'\left(\sum_{j=0}^{n-1}\left(\rho^{\mathbb{Q}}\right)^j\right)\mu^{\mathbb{Q}}$. The first term on the right-hand side of (A.1) is

$$\begin{aligned}
\mathbb{E}_t^{\mathbb{Q}}[r_{t+n}] &= \mathbb{E}_t^{\mathbb{Q}}[\max(\underline{r}_{t+n} + sp_{t+n}, s_{t+n})] \\
&= \mathbb{E}_t^{\mathbb{Q}}[\max(\underline{r}_{t+n}, s_{t+n} - sp_{t+n}) + sp_{t+n}] \\
&= \sum_{\underline{r}_{t+n}} \mathbb{Q}_t(\underline{r}_{t+n}) \mathbb{E}_t^{\mathbb{Q}}[\max(\underline{r}_{t+n}, s_{t+n} - sp_{t+n})|\underline{r}_{t+n}] + \mathbb{E}_t^{\mathbb{Q}}(sp_{t+n}) \\
&= \sum_{\underline{r}_{t+n}} \mathbb{Q}_t(\underline{r}_{t+n}) \left(\underline{r}_{t+n} + \tilde{\sigma}_n^{\mathbb{Q}} g\left(\frac{\bar{a}_n + b_n' X_t - c_n - d_n sp_t - \underline{r}_{t+n}}{\tilde{\sigma}_n^{\mathbb{Q}}}\right)\right) + c_n + d_n sp_t,
\end{aligned}$$

where the derivation for the last equal sign follows Wu and Xia (2016).
The second term of (A.1) is

$$\begin{aligned}
&\frac{1}{2}\left(\mathbb{V}\mathrm{ar}_t^{\mathbb{Q}}\left[\sum_{j=1}^{n} r_{t+j}\right] - \mathbb{V}\mathrm{ar}_t^{\mathbb{Q}}\left[\sum_{j=1}^{n-1} r_{t+j}\right]\right) \\
\approx\ & \mathbb{Q}_t(s_{t+n} - sp_{t+n} \geq \underline{r}_{t+n}) \times \frac{1}{2}\left(\mathbb{V}\mathrm{ar}_t^{\mathbb{Q}}\left[\sum_{j=1}^{n} s_{t+j}\right] - \mathbb{V}\mathrm{ar}_t^{\mathbb{Q}}\left[\sum_{j=1}^{n-1} s_{t+j}\right]\right) \\
=\ & \sum_{\underline{r}_{t+n}} \mathbb{Q}_t(\underline{r}_{t+n})\mathbb{Q}_t(s_{t+n} - sp_{t+n} \geq \underline{r}_{t+n} | \underline{r}_{t+n}) \times \frac{1}{2}\left(\mathbb{V}\mathrm{ar}_t^{\mathbb{Q}}\left[\sum_{j=1}^{n} s_{t+j}\right] - \mathbb{V}\mathrm{ar}_t^{\mathbb{Q}}\left[\sum_{j=1}^{n-1} s_{t+j}\right]\right) \\
=\ & \sum_{\underline{r}_{t+n}} \mathbb{Q}_t(\underline{r}_{t+n})\Phi\left(\frac{\bar{a}_n + b_n' X_t - c_n - d_n sp_t - \underline{r}_{t+n}}{\tilde{\sigma}_n^{\mathbb{Q}}}\right) \times (\bar{a}_n - a_n),
\end{aligned}$$

where the first approximation sign and last equal sign follow Wu and Xia (2016).
Adding them together yields (4.2):

$$\begin{aligned}
f_{nt} \approx\ & \sum_{\underline{r}_{t+n}} \mathbb{Q}_t(\underline{r}_{t+n})\left(\underline{r}_{t+n} + \tilde{\sigma}_n^{\mathbb{Q}} g\left(\frac{a_n + b_n' X_t - c_n - d_n sp_t - \underline{r}_{t+n}}{\tilde{\sigma}_n^{\mathbb{Q}}}\right)\right) + c_n + d_n sp_t \\
=\ & \sum_{\underline{r}_{t+n}} \mathbb{Q}_t(\underline{r}_{t+n})\left(\underline{r}_{t+n} + c_n + d_n sp_t + \tilde{\sigma}_n^{\mathbb{Q}} g\left(\frac{a_n + b_n' X_t - c_n - d_n sp_t - \underline{r}_{t+n}}{\tilde{\sigma}_n^{\mathbb{Q}}}\right)\right),
\end{aligned}$$

where the approximation follows Wu and Xia (2016).

Appendix B Estimation

We apply the algorithm of Kim (1994) to our model. Stack the observation equation in (4.6) for all maturities together with (4.5):

$$F_t^o = F(X_t, sp_t, r_t^d, \Xi_t) + \tilde{\eta}_t, \text{ where } \tilde{\eta}_t \sim N(0, \omega^2 I_8).$$

Define $\mathcal{Y}_t \equiv \{F_{1:t}^o, r_{1:t}^d, sp_{1:t}\}$, and $\Xi_t \equiv \{\Delta_t, \Delta_t^l\}$.

Step 1: Approximate the conditional distribution of X_t with $X_t|\Xi_t, \mathcal{Y}_t \sim N(\hat{X}_{t|t}^{\Xi_t}, P_{t|t}^{\Xi_t})$. We initialize $\hat{X}_{0|0}^{s_0} = (I_3 - \rho)^{-1}\mu$, $vec(P_{0|0}^{s_0}) = (I_9 - (\rho \otimes \rho))^{-1} vec(\Sigma\Sigma')$, and $\mathbb{P}(s_0)$ follows a discrete uniform distribution.

We apply the extended Kalman filter as follows:

$$\begin{aligned}
\hat{X}_{t+1|t}^{\Xi_{t+1},\Xi_t} &= \mu + \rho \hat{X}_{t|t}^{\Xi_t}, && \text{(B.1)}\\
P_{t+1|t}^{\Xi_{t+1},\Xi_t} &= \rho P_{t|t}^{\Xi_t} \rho' + \Sigma\Sigma', && \text{(B.2)}\\
\tilde{\eta}_{t+1|t}^{\Xi_{t+1},\Xi_t} &= F_{t+1}^o - F(\hat{X}_{t+1|t}^{\Xi_{t+1},\Xi_t}, sp_{t+1}, r_{t+1}^d, \Xi_{t+1}), && \text{(B.3)}\\
H_{t+1|t}^{\Xi_{t+1},\Xi_t} &= \left(\left. \frac{\partial F(X_{t+1}, sp_{t+1}, r_{t+1}^d, \Xi_{t+1})}{\partial X_{t+1}'} \right|_{X_{t+1}=\hat{X}_{t+1|t}^{\Xi_{t+1},\Xi_t}} \right)', && \text{(B.4)}\\
K_{t+1|t}^{\Xi_{t+1},\Xi_t} &= P_{t+1|t}^{\Xi_{t+1},\Xi_t} H_{t+1|t}^{\Xi_{t+1},\Xi_t} \left((H_{t+1|t}^{\Xi_{t+1},\Xi_t})' P_{t+1|t}^{\Xi_{t+1},\Xi_t} H_{t+1|t}^{\Xi_{t+1},\Xi_t} + \omega I_8 \right)^{-1}, && \text{(B.5)}\\
\hat{X}_{t+1|t+1}^{\Xi_{t+1},\Xi_t} &= \hat{X}_{t+1|t}^{\Xi_{t+1},\Xi_t} + K_{t+1|t}^{\Xi_{t+1},\Xi_t} \tilde{\eta}_{t+1|t}^{\Xi_{t+1},\Xi_t}, && \text{(B.6)}\\
P_{t+1|t+1}^{\Xi_{t+1},\Xi_t} &= \left(I_3 - K_{t+1|t}^{\Xi_{t+1},\Xi_t} (H_{t+1|t}^{\Xi_{t+1},\Xi_t})' \right) P_{t+1|t}^{\Xi_{t+1},\Xi_t}. && \text{(B.7)}
\end{aligned}$$

Note we will write out $X_{t+1|t+1}^{\Xi_{t+1}}$ and $P_{t+1|t+1}^{\Xi_{t+1}}$ in terms of $X_{t+1|t+1}^{\Xi_{t+1},\Xi_t}$ and $P_{t+1|t+1}^{\Xi_{t+1},\Xi_t}$ in Step 3 to complete the iteration. The likelihood for bond prices at $t+1$ is

$$\begin{aligned}
& \mathbb{P}(F_{t+1}^o | r_{t+1}^d, sp_{t+1}, \mathcal{Y}_t, \Xi_{t+1}, \Xi_t) \\
= & \left(2\pi \left| (H_{t+1|t}^{\Xi_{t+1},\Xi_t})' P_{t+1|t}^{\Xi_{t+1},\Xi_t} H_{t+1|t}^{\Xi_{t+1},\Xi_t} + \omega I_8 \right| \right)^{-1/2} \\
& \exp\left(-\frac{1}{2} (\tilde{\eta}_{t+1|t}^{\Xi_{t+1},\Xi_t})' \left| (H_{t+1|t}^{\Xi_{t+1},\Xi_t})' P_{t+1|t}^{\Xi_{t+1},\Xi_t} H_{t+1|t}^{\Xi_{t+1},\Xi_t} + \omega I_8 \right|^{-1} \tilde{\eta}_{t+1|t}^{\Xi_{t+1},\Xi_t} \right). \qquad \text{(B.8)}
\end{aligned}$$

Step 2: We compute the distribution $\mathbb{P}(\Xi_{t+1}, |\mathcal{Y}_{t+1})$ as follows:

$$\mathbb{P}(\Xi_{t+1}|\mathcal{Y}_{t+1}) = \sum_{\Xi_t} \mathbb{P}(\Xi_{t+1}, \Xi_t | \mathcal{Y}_{t+1}), \qquad \text{(B.9)}$$

where

$$\begin{aligned}
\mathbb{P}(\Xi_{t+1}, \Xi_t | \mathcal{Y}_{t+1}) &= \frac{\mathbb{P}(F_{t+1}^o, r_{t+1}^d, sp_{t+1}, \Xi_{t+1}, \Xi_t | \mathcal{Y}_t)}{\mathbb{P}(F_{t+1}^o, r_{t+1}^d, sp_{t+1} | \mathcal{Y}_t)} \\
&= \frac{\mathbb{P}(F_{t+1}^o, r_{t+1}^d, sp_{t+1} | \Xi_{t+1}, \Xi_t, \mathcal{Y}_t) \mathbb{P}(\Xi_{t+1}, \Xi_t | \mathcal{Y}_t)}{\mathbb{P}(F_{t+1}^o, r_{t+1}^d, sp_{t+1} | \mathcal{Y}_t)} \\
&= \frac{\mathbb{P}(F_{t+1}^o, r_{t+1}^d, sp_{t+1} | \Xi_{t+1}, \Xi_t, \mathcal{Y}_t) \mathbb{P}(\Xi_{t+1}, \Xi_t | \mathcal{Y}_t)}{\sum_{\Xi_{t+1},\Xi_t} \mathbb{P}(F_{t+1}^o, r_{t+1}^d, sp_{t+1} | \Xi_{t+1}, \Xi_t, \mathcal{Y}_t) \mathbb{P}(\Xi_{t+1}, \Xi_t | \mathcal{Y}_t)}. \qquad \text{(B.10)}
\end{aligned}$$

We compute $\mathbb{P}(\Xi_{t+1}, \Xi_t | \mathcal{Y}_t)$ as follows:

$$\begin{aligned}
\mathbb{P}(\Xi_{t+1}, \Xi_t | \mathcal{Y}_t) &= \mathbb{P}(\Xi_{t+1} | \Xi_t) \mathbb{P}(\Xi_t | \mathcal{Y}_t) \\
&= \mathbb{P}(\Delta_t | \Delta_{t-1}, \Delta_{t-1}^l) \mathbb{P}(\Delta_t^l | \Delta_{t-1}^l) \mathbb{P}(\Xi_t | \mathcal{Y}_t), \qquad \text{(B.11)}
\end{aligned}$$

where the first two terms are given by the $\mathbb{P}$ version of (2.4) and (2.5), respectively. We compute $\mathbb{P}(F^o_{t+1}, r^d_{t+1}, sp_{t+1}|\mathcal{Y}_t, \Xi_{t+1}, \Xi_t)$ in (B.10) as follows:

$$\begin{aligned}\mathbb{P}(F^o_{t+1}, r^d_{t+1}, sp_{t+1}|\mathcal{Y}_t, \Xi_{t+1}, \Xi_t) &= \mathbb{P}(F^o_{t+1}|r^d_{t+1}, sp_{t+1}, \mathcal{Y}_t, \Xi_{t+1}, \Xi_t) \\ &\quad \mathbb{P}(r^d_{t+1}|sp_{t+1}, \mathcal{Y}_t, \Xi_{t+1}, \Xi_t)\mathbb{P}(sp_{t+1}|\mathcal{Y}_t, \Xi_{t+1}, \Xi_t). \quad \text{(B.12)}\end{aligned}$$

The first term in (B.12) is calculated in (B.8). Using (2.2), the second term is

$$\mathbb{P}(r^d_{t+1}|sp_{t+1}, \mathcal{Y}_t, \Xi_{t+1}, \Xi_t) = \mathbb{P}(r^d_{t+1}|r^d_t, \Delta_t) = \mathbf{1}_{\{r^d_{t+1}=r^d_t\}} \times (1-\alpha_{1,\Delta_t}) + \mathbf{1}_{\{r^d_{t+1}=r^d_t-0.1\%\}} \times \alpha_{1,\Delta_t}.$$

Using the $\mathbb{P}$ version of (4.1), the third term in (B.12) is

$$\mathbb{P}(sp_{t+1}|\mathcal{Y}_t, \Xi_{t+1}, \Xi_t) = \mathbb{P}(sp_{t+1}|sp_t) = (2\pi\sigma^2_{sp})^{-1/2} \exp\left(-\frac{(sp_{t+1}-\mu_{sp}-\rho_{sp}sp_t)^2}{2\sigma^2_{sp}}\right).$$

With (B.11) and (B.12), we can also calculate the log likelihood for period $t+1$

$$\mathbb{P}(F^o_{t+1}, r^d_{t+1}, sp_{t+1}|\mathcal{Y}_t) = \sum_{\Xi_{t+1}, \Xi_t} \mathbb{P}(F^o_{t+1}, r^d_{t+1}, sp_{t+1}|\mathcal{Y}_t, \Xi_{t+1}, \Xi_t)\mathbb{P}(\Xi_{t+1}, \Xi_t|\mathcal{Y}_t). \quad \text{(B.13)}$$

Step 3: Finally, we can complete the recursion in (B.1) - (B.7) with

$$\begin{aligned}\hat{X}^{\Xi_{t+1}}_{t+1|t+1} &= \frac{\sum_{\Xi_t} \mathbb{P}(\Xi_{t+1}, \Xi_t|\mathcal{Y}_{t+1})\hat{X}^{\Xi_{t+1}, \Xi_t}_{t+1|t+1}}{\mathbb{P}(\Xi_{t+1}|\mathcal{Y}_{t+1})}, \\ P^{\Xi_{t+1}}_{t+1|t+1} &= \frac{\sum_{\Xi_t} \mathbb{P}(\Xi_{t+1}, \Xi_t|\mathcal{Y}_{t+1}) \left(P^{\Xi_{t+1}, \Xi_t}_{t+1|t+1} + (\hat{X}^{\Xi_{t+1}}_{t+1|t+1} - \hat{X}^{\Xi_{t+1}, \Xi_t}_{t+1|t+1})(\hat{X}^{\Xi_{t+1}}_{t+1|t+1} - \hat{X}^{\Xi_{t+1}, \Xi_t}_{t+1|t+1})'\right)}{\mathbb{P}(\Xi_{t+1}|\mathcal{Y}_{t+1})},\end{aligned}$$

where $\hat{X}^{\Xi_{t+1}, \Xi_t}_{t+1|t+1}$ and $P^{\Xi_{t+1}, \Xi_t}_{t+1|t+1}$ are calculated in (B.6) and (B.7), and $\mathbb{P}(\Xi_{t+1}|\mathcal{Y}_{t+1})$ is from (B.9).

Log likelihood The log likelihood is $\sum_{t=0}^{T-1} \log\left(\mathbb{P}(F^o_{t+1}, r^d_{t+1}, sp_{t+1}|\mathcal{Y}_t)\right)$. At the ELB, $\mathbb{P}(F^o_{t+1}, r^d_{t+1}, sp_{t+1}|\mathcal{Y}_t)$ is calculated in (B.13). Before the ELB, sp_t, r^d_t, Ξ_t are all irrelevant, and $\mathbb{P}(F^o_{t+1}, r^d_{t+1}, sp_{t+1}|\mathcal{Y}_t) = \mathbb{P}(F^o_{t+1}|F^o_t)$, which is computed by (B.8) through the extended Kalman filter in (B.1) - (B.7) by ignoring Ξ_t, Ξ_{t+1}.

Appendix C Alternative models

Table C.1: Model specifications

	short description	full description
M_{main}	main model	The main model specified in Sections 2-3.
M_{Δ_t}	model with only Δ_t	Impose $\alpha_{00,\Delta_t^l} = \alpha_{00}, \alpha_{11,\Delta_t^l} = \alpha_{11}, \alpha^{\mathbb{Q}}_{00,\Delta_t^l} = \alpha^{\mathbb{Q}}_{00}, \alpha^{\mathbb{Q}}_{11,\Delta_t^l} = \alpha^{\mathbb{Q}}_{11}$ on our main model.
M_{S-TV}	benchmark shadow rate model with time-varying lower bound and myopic agents	$\underline{r}_t = r_t^d$ for ELB. But agents are not forward looking, and think the future lower bound would stay where it is today. Also, $sp_t = 0$. This specification is similar to Lemke and Vladu (2016), and Kortela (2016).
M_{S-0}	benchmark shadow rate model with a constant lower bound at 0	This model has a constant lower bound at 0, and $sp_t = 0$. This is similar to Christensen and Rudebusch (2014), Wu and Xia (2016), and Bauer and Rudebusch (2016).
$M_{S-.4}$	benchmark shadow rate model with a constant lower bound at -0.4%	This model is the same as the previous one, except the lower bound is changed to -0.4%.
M_G	benchmark Gaussian affine term structure model	In this model, $r_t = \Xi_t$.